

Dynamical decoupling of a single-electron spin at room temperature

Boris Naydenov,^{1,*} Florian Dolde,¹ Liam T. Hall,² Chang Shin,³ Helmut Fedder,¹
Lloyd C. L. Hollenberg,² Fedor Jelezko,¹ and Jörg Wrachtrup¹

¹*3rd Physics Institute and Research Center SCOPE, University of Stuttgart, D-70659 Stuttgart, Germany*

²*Centre for Quantum Computer Technology, School of Physics, University of Melbourne, Victoria 3010, Australia*

³*National Biomedical Center for Advanced ESR Technology, Department of Chemistry and Chemical Biology,*

Cornell University, Ithaca, New York 14853, USA

(Received 30 November 2010; published 2 February 2011)

Here we report the increase of the coherence time T_2 of a single-electron spin at room temperature by using dynamical decoupling. We show that the Carr-Purcell-Meiboom-Gill (CPMG) pulse sequence can prolong the T_2 of a single nitrogen-vacancy center in diamond up to 2.44 ms compared to the Hahn echo measurement where $T_2 = 400 \mu\text{s}$. Moreover, by performing spin-locking experiments we demonstrate that with CPMG the maximum possible T_2 is reached. On the other hand, we do not observe a strong increase of the coherence time in nanodiamonds, possibly due to the short spin-lattice relaxation time $T_1 = 100 \mu\text{s}$ (compared to $T_1 = 5.93$ ms in bulk). An application for detecting low magnetic fields is demonstrated, where we show that the sensitivity using the CPMG method is improved by about a factor of 2 compared to the Hahn echo method.

DOI: [10.1103/PhysRevB.83.081201](https://doi.org/10.1103/PhysRevB.83.081201)

PACS number(s): 76.30.Mi, 61.72.jn, 76.60.Lz, 76.70.Hb

The negatively charged nitrogen-vacancy (NV^-) centers in diamond (later denoted as NV) are one of the most promising quantum bits (qubits) for a scalable solid-state quantum computer. Single NVs can be addressed optically even at room temperature,^{1,2} and the first quantum registers containing several qubits have been demonstrated.³⁻⁵ One of the main advantages of the NV centers is their long coherence time T_2 at room temperature, reaching almost 2 ms in ultrapure isotopically enriched ^{12}C diamond,⁶ permitting the detection of weak magnetic fields^{7,8} reaching a sensitivity of $4 \frac{\text{nT}}{\sqrt{\text{Hz}}}$.⁶ Recently, a wide field approach has been demonstrated to have sensitivity of $20 \frac{\text{nT}}{\sqrt{\text{Hz}}}$, where an ensemble of NVs are used as sensors.⁹

It is of crucial importance to develop new methods for increasing the coherence time of NV in an environment that is not ultrapure. We will consider the terms decoherence and dephasing interchangeable, although this is not strictly correct (see, for example, Ref. 10). In this Rapid Communication we demonstrate that T_2 of an NV center in a bulk diamond can be increased by a factor of 6 using the Carr-Purcell-Meiboom-Gill (CPMG) pulse sequence. The CPMG sequence is widely used in the NMR community^{11,12} and was recently rediscovered in the context of quantum computing theory¹³ and experiment,^{14,15} and has been proposed as a method for increasing the sensitivity of NV-based magnetometers.^{16,17} Although common in the field of NMR, this sequence has not found wide application in electron spin resonance (ESR), as relatively few reports are known (e.g., Refs. 18 and 19).

The NV center consists of a substitutional nitrogen atom and a neighboring carbon vacancy [Fig. 1(a)]. The system has a triplet ground state, as described by the following Hamiltonian ($\hbar = 1$):

$$H = [\omega_L + \omega_e(t)]S_z + D[S_z^2 + \frac{1}{3}S(S+1)] + H_{\text{HF}}, \quad (1)$$

where $\omega_L = g_e \mu_B B_0$ is the Larmor frequency, $\omega_e(t) = g_e \mu_B B_e(t)$ represents the magnetic field fluctuations in the environment which cause decoherence, g_e is the g factor of the $S = 1$ NV electron spin, μ_B is the Bohr magneton, B_0

is the applied constant magnetic field, $D = 2.88$ GHz is the zero-field splitting, and H_{HF} is the hyperfine interaction to the nitrogen nucleus, which may be ignored in the present context. A small magnetic field $B_0 \approx 15$ G is aligned along the NV quantization axis (defined by the D, z axis in the rotating frame) in order to split the $m_s = \pm 1$ levels. Aligning the field is important since T_2 depends on the orientation of B_0 , where the maximum is reached for B_0 parallel to the NV axis.^{20,21}

The magnetic field at the NV center can be written as $B(t) = B_0 + B_e(t)$, where its mean value and its standard deviation are $\langle B \rangle = B_0$ and $B'(t) = \sqrt{\langle B^2 \rangle - B_0^2}$, respectively. If the fluctuation rate of $B_e(t)$ is $f_e = 1/\tau_e$, it has been recently shown²² that in the case of a slow fluctuation limit and for all t [$1/\tau_e g_e \mu_B B'(t) \gg 1$], $B(t)$ can be expanded as a Taylor series:

$$B(t) = \sum_{k=0}^N \frac{1}{k!} \frac{d^k B}{dt^k} \Big|_{t_0} (t - t_0)^k \equiv \sum_{k=0}^N a_k (t - t_0)^k, \quad (2)$$

where each a_k represents a different dephasing channel.

We consider the Hahn echo pulse sequence depicted in Fig. 2(b) and its effect on Eq. (2). A laser pulse with wavelength $\lambda = 532$ nm and $2 \mu\text{s}$ duration is used to polarize the NV into the $m_s = 0$ state [Fig. 2(a)] and read out the population difference between $m_s = 0$ and $m_s = 1$ states [Fig. 1(b)].¹ A microwave (MW) $\pi/2$ pulse resonant with the $m_s = 0 \rightarrow m_s = +1$ transition is applied along the y axis in the rotating frame. The NV is transformed into the superposition state $|\psi\rangle = 1/\sqrt{2}(|0\rangle + |1\rangle)$ or equivalently, the effect of the MW pulse is to transfer the equilibrium spin magnetization M from z to the x axis in the rotating frame. Inhomogeneities [a_0 in Eq. (2)] and quasistatic fluctuations $B(t)$ due to the ^{13}C spin bath in the surroundings of NV cause the decay of $|\psi\rangle$ with decay function (for long t) e^{-t/T_2^*} , a process known as free induction decay (FID). The evolution of the system is described by the Hamiltonian $H_{\text{evol}} = \omega(t)S_z$ and the evolution operator $U_{\text{evol}} = e^{-\int H_{\text{evol}} dt}$. The application of a π pulse at

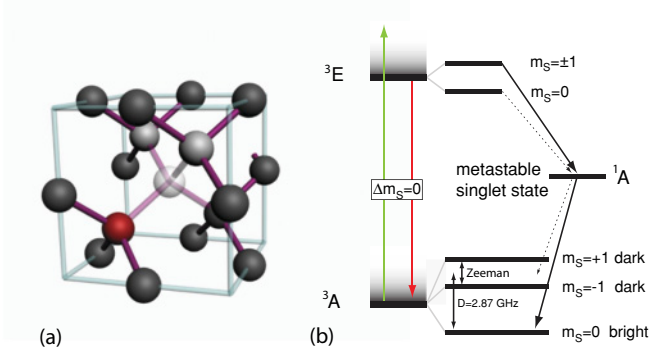


FIG. 1. (Color online) (a) Schematic view of the NV center in diamond. (b) Energy-level scheme of NV. A green laser excites the NV to 3E , from which it can fall back to 3A or undergo intersystem crossing to a metastable state 1A . From there it decays to the $m_s = 0$ ground state, thus polarizing the electron spin.

time τ inverts the sign of H_{evol} , resulting in a “refocusing” of the spin coherence at time 2τ . Strictly speaking, the contribution of a_0 in the dephasing is completely removed, whereas the contribution from high-order terms is suppressed via^{17,22}

$$a_k \mapsto (1 - 2^{-k})a_k. \quad (3)$$

The final $\pi/2$ pulse is used to transfer the coherence into the population difference, which is read out optically. With longer τ , the effects on the phase coherence of low-frequency fluctuations in the environment become more pronounced. Such effects can be mitigated significantly with the application of a CPMG pulse sequence¹³ [Fig. 2(c)] in which a series of π pulses are applied at times $(2n + 1)\tau$ for $n = 0, 1, \dots, N$, yielding multiple echoes at times $(2n + 2)\tau$. The lower index in the rotation angle of the MW pulse represents the phase of the MW, where 0° implies the alignment of the MW magnetic fields $B_1 \parallel y$ and $90^\circ B_1 \parallel x$. Shifting the phase of the π pulse train by 90° is important for suppressing errors in the pulse

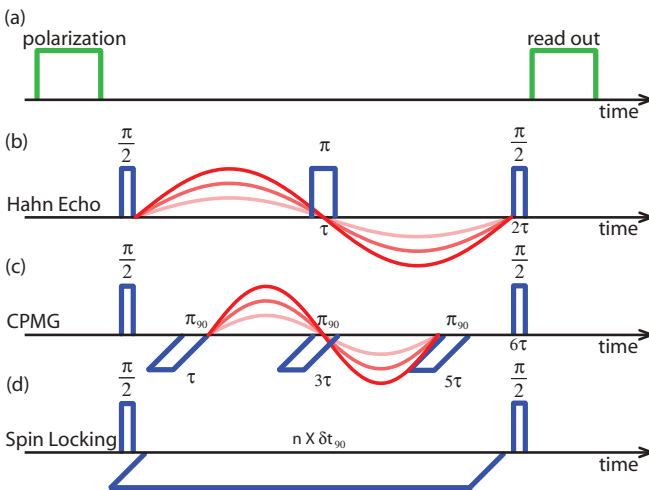


FIG. 2. (Color online) Pulse sequences used in the experiments. The curved lines represent the applied ac magnetic field. (a) Optical polarization and readout of the NV electron spin, (b) Hahn echo, (c) CPMG, and (d) spin locking (see text for more details).

length.¹² Experimentally we realized this by splitting the MW using a 90° hybrid (minicircuits zx10Q-2-34-5+) into two channels. A MW switch (minicircuits ZASWA-2-SODR) for each channel was used for creating the MW pulses.

The quantum phase accumulated by the NV spin $\Delta\phi$ is proportional to the time integral of the magnetic field $B(t)$ from Eq. (2). If m pulses are applied at the instants t_1, t_2, \dots, t_m , the effect of the pulse sequence on the phase shift will be

$$\Delta\phi = \frac{g_e \mu_B}{\hbar} \left(\int_0^{t_1} - \int_{t_1}^{t_2} + \dots + (-1)^m \int_{t_m}^{\tau} \right) B(t) dt.$$

The effect of an arbitrary sequence of pulses on the j th term in the Taylor expansion is then

$$a_j \mapsto a_j \frac{(\int_0^{t_1} - \int_{t_1}^{t_2} \dots + (-1)^m \int_{t_m}^{\tau}) t^j dt}{\int_0^{\tau} t^j dt}.$$

For a CPMG sequence, the time of application of the j th pulse in an n pulse sequence is $t_j = \frac{2j-1}{2n}\tau$, where $j \in \{1, 2, \dots, n\}$. For 1 pulse (Hahn echo), the effect on the k th Taylor term is given in Eq. (3), and in general, for 2, 3, and n pulses, we have

$$\begin{aligned} 2 a_k &\mapsto a_k \frac{1}{4^{k+1}} [2 - 2(3)^{k+1} + 4^{k+1}], \\ 3 a_k &\mapsto a_k \frac{1}{6^{k+1}} [2 - 2(3)^{k+1} + 2(5)^{k+1} - 6^{k+1}], \\ &\vdots \\ n a_k &\mapsto a_k \frac{1}{(2n)^{k+1}} [2 + (-1)^n (2n)^{k+1} \\ &\quad + 2 \sum_{j=1}^{n-1} (-1)^j (2j+1)^{k+1}]. \end{aligned}$$

If $a_k \ll 1/\tau$ (τ being the interpulse distance), the influence of a_k on the coherence is eliminated. In the limit of $\tau \rightarrow 0$ we arrive at the spin-locking regime [Fig. 2(d)] where the system does not evolve freely, but it is constantly driven by the MW field. In this case the spin magnetization is “locked” to the x axis in the rotating frame and it decays with time constant $T_{1\rho}$ determined by the noise spectral density $J(\omega_1)$, where $\omega_1 = g\mu_B B_1/\hbar$ is the Rabi frequency with B_1 the MW magnetic field. For very high MW power $\omega_1 \approx \omega_L$, $T_{1\rho}$ approaches the spin-lattice relaxation time T_1 proportional to $J(\omega_L)$. Since the decoherence channels do not influence the transverse magnetization anymore (the system does not evolve freely), $T_{1\rho}$ can be considered as the upper limit for T_2 measured by any multiple pulse (decoupling) sequence, if the same MW power is used.

The data from the decoupling experiments are plotted in Fig. 3. The diamond sample used for these measurements has been chemical vapor deposition (CVD) grown (element 6) with natural ${}^{13}\text{C}$ abundance (about 1%) and low nitrogen impurity concentration (below 1 ppb). According to theoretical calculations the Hahn echo decays as $e^{-(2\tau/T_2)^3}$,²³ which was fitted to the data. From the fit we obtain $T_2 = 400 \mu\text{s}$, which is in very good agreement with the value predicted

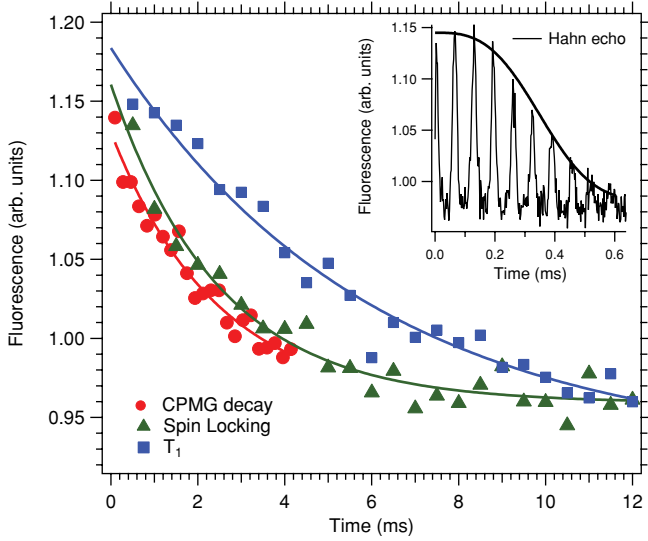


FIG. 3. (Color online) Hahn echo decay (inset, $T_2 = 0.4 \pm 0.16$ ms), CPMG (circles, $T_2^{\text{CPMG}} = 2.44 \pm 0.44$ ms), spin locking (triangles, $T_{1\rho} = 2.47 \pm 0.27$ ms), and spin-lattice relaxation (squares, $T_1 = 5.93 \pm 0.7$ ms). The solid curves are fits to the data (see text).

from the theory $T_2^{\text{theory}} = 400 \mu\text{s}$ for decoherence caused by fluctuations in the ^{13}C ($I = 1/2$, 1% concentration) spin bath.¹⁷ This electron-nuclear coupling results in the electron spin envelope modulation (ESEEM) at the Larmor frequency ω_C of ^{13}C shown in Fig. 3, as described in detail by Van Oort *et al.* and Childress *et al.*²⁵ For the CPMG measurement τ was set to be at the maximum of the Hahn echo revivals, thus providing a maximum signal.¹⁸ If $\tau < 2\pi/\omega_C$, we also observed oscillations in the echo train (data not shown). For the CPMG experiment the theory predicts exponential decay with an increase of the decay constant as $T_2^{\text{CPMG}} = (2n)^{2/3}T_2$, where n is the number of pulses.²⁴ We observe that $T_2^{\text{CPMG}} = 2.44$ ms, which is about six times longer than T_2 , whereas a factor of 32 ($n = 90$) is expected from the theoretical formula. Spin-locking decay measurements reveal $T_{1\rho} = 2.47$ ms, a value close to the spin-lattice relaxation time $T_1 = 5.93$ ms in this sample. Thus we have $T_2^{\text{CPMG}} = T_{1\rho} \sim T_1$, meaning that we are able to suppress the decoherence channels almost to the limit imposed by the relaxation processes T_1 . Identical experiments were performed with nanodiamonds [ND, synthetic “metal bond”-type diamond powders (SYP) from Van Moppes, average diameter 30 nm], where the CPMG technique improves the T_2 only by a factor of 2—from $2.1 \mu\text{s}$ to $4.8 \mu\text{s}$. From spin-locking measurements we extract $T_{1\rho} = 13 \mu\text{s}$, suggesting that there is a strong source of decoherence and relaxation in ND, which also limits T_1 to $100 \mu\text{s}$. This result could be explained by the dense electron-spin bath surrounding the NV in ND.²⁶

For the magnetometry experiments a gold microstructure was directly deposited on the diamond to provide MW and ac magnetic fields. The latter was created by an arbitrary wave form generator (Tektronix AWG 2041). The superposition state $|\psi\rangle$ during its free evolution accumulates a relative phase $\Delta\Phi$ which is used for the detection of small magnetic fields.^{8,16}

The sensitivity is proportional to $\sqrt{T_2}$ and the collected phase is given by

$$\Delta\Phi = \int_0^\tau \Delta\omega dt = \frac{ge\mu_B}{\hbar} \int_0^\tau B(t) dt, \quad (4)$$

where $\Delta\omega$ is the shift of the Larmor frequency. The π pulse in the Hahn echo changes the sign of the collected phase and $\Delta\Phi_{\text{Hahn}}$ is then

$$\Delta\Phi_{\text{Hahn}} = \frac{ge\mu_B}{\hbar} \int_0^\tau B(t) dt - \frac{ge\mu_B}{\hbar} \int_\tau^{2\tau} B(t) dt. \quad (5)$$

This measurement scheme can be used to detect an ac magnetic field with frequency ($\frac{1}{2\tau}$) and synchronized phase.⁷ For sensing with the CPMG pulse sequence, the frequency has to be set to $\frac{1}{4\tau}$ (see Fig. 2). In this case $\Delta\Phi_{\text{CPMG}}$ for n π pulses is

$$\begin{aligned} \Delta\Phi_{\text{CPMG}} &= \frac{ge\mu_B}{\hbar} \left(\int_0^\tau B(t) dt \sum_{n=1,3,5,\dots} \int_{(2n-1)\tau}^{(2n+1)\tau} B(t) dt \right. \\ &\quad \left. - \sum_{n=2,4,6,\dots} \int_{(2n-1)\tau}^{(2n+1)\tau} B(t) dt + (-1)^n \int_{(2n+1)\tau}^{(2n+2)\tau} B(t) dt, \right) \end{aligned}$$

The detected signal is then proportional to $\cos(\Delta\Phi)$. The lowest detectable magnetic field δB_{min} is determined by the change of the measured signal and its error, where the steepest change in the signal is considered to maximize sensitivity. The error is given by the shot-noise limitation of the collected photons. δB_{min} can be calculated by

$$\delta B_{\text{min}} = \frac{\sigma_{\text{sn}}}{\delta S}, \quad (6)$$

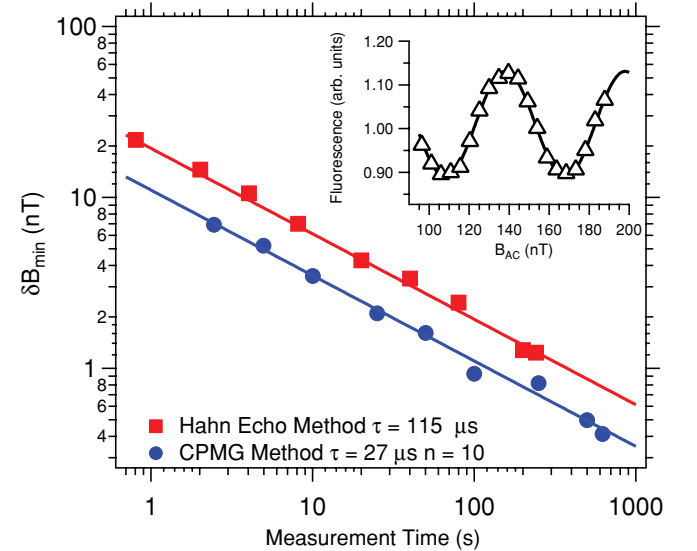


FIG. 4. (Color online) The graph represents δB_{min} as a function of the total measurement time per data point for Hahn echo and CPMG based magnetometry. The blue line denotes fits with the shot-noise limit $\delta B_{\text{min}} = \frac{k}{\sqrt{t}}$. The inset shows the oscillations in the fluorescence intensity due to the applied ac magnetic field.

where σ_{sn} is the uncertainty in the measured data point (determined by the standard deviation) and δS is the maximum slope of the signal change [$\delta S = \frac{\Delta S}{\Delta B}$ with ΔB being the increase of the applied magnetic field and ΔS the change of the fluorescence (Fig. 4, inset)]. The dependence of δB_{\min} on σ_{sn} is depicted in Fig. 4, where $\tau = 115 \mu\text{s}$ was chosen for the Hahn echo based method. For the CPMG detection scheme $n = 10$ and $\tau = 27 \mu\text{s}$ was used. Increasing the number of pulses above ten did not improve the sensitivity, most likely due to noise in the applied ac magnetic field. Nevertheless, the application of the CPMG technique significantly reduces δB_{\min} , as can be seen in Fig. 4. The lowest value we measured is $\delta B_{\min} = 0.4 \text{ nT}$, which corresponds to the magnetic field created by a proton at a distance about 5 nm away from the NV.¹⁶ The fit of the shot-noise limit $\delta B_{\min} = \frac{k}{\sqrt{t}}$ reveals a sensitivity k of $k_{\text{Hahn}} = 19.4 \pm 0.4 \frac{\text{nT}}{\sqrt{\text{Hz}}}$ and $k_{\text{CPMG}} = 11.0 \pm 0.2 \frac{\text{nT}}{\sqrt{\text{Hz}}}$.

We have demonstrated the possibility of extending the coherence times of a single NV center in diamond via the application of a CPMG pulse sequence. Using this, we have managed to demonstrate improved ac magnetic field sensitivity compared to the Hahn echo method. These results pave the way toward the detection of single-electron spins at ambient conditions, which has wide applications in the life sciences and nanotechnology. Results closely related to this work have been recently reported by de Lange *et al.*^{27,28} (where the main dephasing source is the nitrogen electron spin bath) and Ryan *et al.*²⁹

We are grateful to Gopalakrishnan Balasubramanian and Florian Remppl for useful discussions. This work is supported by the EU (QAP, EQUIND, NEDQIT, SOLID), DFG (SFB/TR21 and FOR730, FOR1482), BMBF (EPHQUAM and KEPHOSI) and Landesstiftung BW. L.C.L.H. and L.T.H. acknowledge support of the Australian Research Council.

*b.naydenov@physik.uni-stuttgart.de

¹F. Jelezko, T. Gaebel, I. Popa, A. Gruber, and J. Wrachtrup, *Phys. Rev. Lett.* **92**, 076401 (2004).

²F. Jelezko, T. Gaebel, I. Popa, M. Domhan, A. Gruber, and J. Wrachtrup, *Phys. Rev. Lett.* **93**, 130501 (2004).

³M. V. G. Dutt *et al.*, *Science* **316**, 1312 (2007).

⁴P. Neumann *et al.*, *Science* **320**, 1326 (2008).

⁵P. Neumann *et al.*, *Nat. Phys.* **6**, 249 (2010).

⁶G. Balasubramanian *et al.*, *Nat. Mater.* **8**, 383 (2009).

⁷J. R. Maze *et al.*, *Nature (London)* **455**, 644 (2008).

⁸G. Balasubramanian *et al.*, *Nature (London)* **455**, 648 (2008).

⁹S. Steinert *et al.*, *Rev. Sci. Instrum.* **80**, 043705 (2010).

¹⁰W. H. Zurek, *Rev. Mod. Phys.* **75**, 715 (2003).

¹¹H. Y. Carr and E. M. Purcell, *Phys. Rev.* **94**, 630 (1956).

¹²S. Meiboom and D. Gill, *Rev. Sci. Instrum.* **29**, 688 (1958).

¹³W. M. Witzel and S. Das Sarma, *Phys. Rev. Lett.* **98**, 077601 (2007); L. Cywinski, R. M. Lutchyn, C. P. Nave, and S. Das Sarma, *Phys. Rev. B* **77**, 174509 (2008); W. Yang, Z. Y. Wang, and R. B. Liu, *Front. Phys.* **5**, 1 (2010).

¹⁴H. Bluhm *et al.*, *Nat. Phys.*, doi:10.1038/nphys1856 (2010).

¹⁵J. Du *et al.*, *Nature (London)* **461**, 1265 (2009).

¹⁶J. M. Taylor *et al.*, *Nat. Phys.* **4**, 810 (2008).

¹⁷L. T. Hall, C. D. Hill, J. H. Cole, and L. C. L. Hollenberg, *Phys. Rev. B* **82**, 045208 (2010).

¹⁸J. R. Harbridge, S. S. Eaton, and G. R. Eaton, *J. Magn. Reson.* **164**, 44 (2003).

¹⁹C. Van't Hof *et al.*, *Chem. Phys. Lett.* **21**, 437 (1973).

²⁰J. R. Maze, J. M. Taylor, and M. D. Lukin, *Phys. Rev. B* **78**, 094303 (2008).

²¹P. L. Stanwix, L. M. Pham, J. R. Maze, D. LeSage, T. K. Yeung, P. Cappellaro, P. R. Hemmer, A. Yacoby, M. D. Lukin, and R. L. Walsworth, *Phys. Rev. B* **82**, 201201(R) (2010).

²²L. T. Hall, J. H. Cole, C. D. Hill, and L. C. L. Hollenberg, *Phys. Rev. Lett.* **103**, 220802 (2009).

²³R. de Sousa and S. Das Sarma, *Phys. Rev. B* **68**, 115322 (2003).

²⁴R. de Sousa, *Top. Appl. Phys.* **115**, 183 (2009).

²⁵E. Van Oort and M. Glasbeek, *Chem. Phys.* **143**, 131 (1990); L. Childress *et al.*, *Science* **314**, 281 (2006).

²⁶J. Tisler *et al.*, *ACS Nano* **3**, 1959 (2009).

²⁷G. de Lange *et al.*, *Science* **330**, 60 (2010).

²⁸G. de Lange *et al.*, e-print arXiv:1008.4395 (to be published).

²⁹C. A. Ryan, J. S. Hodges, and D. G. Cory, *Phys. Rev. Lett.* **105**, 200402 (2010)